Case study

Sustainability assessment of geopolymer concrete synthesized by slag and corncob ash

Solomon Oyebisi [a],[*], Festus Olutoge [b], Parthiban Kathirvel [c], Increase Oyaotuderekumor [a], David Lawanson [a], Joy Nwani [a], Anthony Ede [a], Rodrigue Kaze [d]

[a] Department of Civil Engineering, Covenant University, Ota, Nigeria
[b] Department of Civil and Environmental Engineering, University of West Indies, Trinidad and Tobago
[c] School of Civil Engineering, SASTRA Deemed University, Thanjavur 613401, India
[d] Laboratory of inorganic applied chemistry, university of Yaoundé I, Yaoundé, Cameroon

ARTICLE INFO

ABSTRACT

Globally, sustainable construction materials are promoted in the construction and building sector due to the high utilization of Portland cement as a conventional binder and its associated energy and environmental impacts. Consequently, geopolymer concrete emerges as a substitute for conventional concrete. This study designed two grades of geopolymer concrete (GPC) strengths (C 30 and 40 MPa) with ground granulated blast furnace slag (GGBFS) and corncob ash (CCA) as alternative binders. The binders, varied at 0–100 wt% of GGBFS by CCA, were activated with sodium hydroxide (SH) and sodium silicate (SS) solutions. After 28 days of curing, the compressive strength of the concrete cubes was determined. Furthermore, the environmental impacts of the concrete constituents were assessed. At the same time, their sustainability and economic indexes were estimated via the Inventory of Carbon and Energy (ICE) within the cradle-to-site confinement. The findings showed that GGBFS-CCA-based geopolymer concrete exhibited lesser environmental impact and higher sustainable and economic efficiency than Portland cement concrete. Thus, these outcomes can be advantageous in achieving a cleaner built milieu and sustainable construction.

1. Introduction

Increasing the use of Portland cement (PC) in the construction industry leads to environmental pollution and high energy use [1,2]. PC is necessary for the manufacturing of concrete in the building and construction industry [3,4]. Due to the high energy requirements and greenhouse gas emissions (GHG), particularly carbon dioxide (CO_2) emissions, this activity is not sustainable. The intensive energy is generated during PC production, contributing about 7% of CO_2 discharges into the atmosphere [5] and 14% of the entire global energy consumption [6]. Furthermore, Perez et al. [7] stated that the production of 1000 kg of cement consumes about 110 kwh of electricity and emits approximately 800 $kgCO_2$. The PC and concrete productions emitted about 54 $GtCO_2$-eq of greenhouse gases in 2017; this is projected to increase in the future [8]. Thus, alternative options are needed to mitigate this action. Among these alternatives is geopolymer concrete (GPC) which has received global attention and garnered vital interest in replacing Portland cement

* Corresponding author.
  E-mail address: solomon.oyebisi@covenantuniversity.edu.ng (S. Oyebisi).

concrete (PCC) fully or partially [9].

Recycling supplementary cementitious materials (SCMs) as an alternative to PC contributes to energy reduction, environmental preservation, and sustainability [10,11]. Replacing PC with about 25–50 wt% of SCMs reduces carbon dioxide emissions, energy, and cost by about 13–22%, 20–67%, and 33–80%, respectively [12,13]. Geopolymer concrete from SCMs such as ground granulated blast furnace slag (GGBFS), corn cob ash (CCA), and fly ash offers mechanical and durability benefits. It yielded higher mechanical performance than PCC [14,15]. Besides, it resisted more acidic and sulfate attacks than PCC [11,16,17].

A global product range of 170–250 metric tonnes of GGBFS is generated annually [18], and the global generation is projected to increase by 15% in 2030 [19]. Approximately 1130,000 MMT of corn were produced in 2017, with Africa and Nigeria producing about 84.2 and 11 MMT, respectively [20]. Presently, in Nigeria, GBFS and corncob have no commercial value. They are discarded as wastes, resulting in environmental problems.

A Life cycle assessment (LCA)-based environmental assessment of fly ash, SF, and gibbsite-based geopolymer paste activated with SH and SS was investigated by Mclellan et al. [21]. The results, including the sum of production and transportation emissions, indicated a 44–64% reduction in CO_2 emissions compared with PC paste. In a further study, Heath et al. [22] reported a 40% reduction in CO_2 emissions when meta-clay GPC was activated with SH and SS solutions compared with PCC. Also, Habert and Ouellet-Plamondon [23] found a 75% reduction in CO_2 emissions when fly ash-GGBFS-based GPC was activated with SH and SS solutions compared with PCC. Similarly, global warming potential (GWP) and global temperature potential (GTP) were reduced to approximately 44.7% when natural volcanic soil-based GPC activated with SH and SS solutions was produced compared with PCC [24].

From the economic viewpoint, Mclellan et al. [21] performed the cost analysis on four geopolymer binders based on production and transportation. In terms of cost performance, geopolymer binders indicated that an enhancement over PC is feasible, with expenses ranging between 7% and 39% more than PC. But, without a carbon price, geopolymer binders are not cost-efficient [21]. However, Refaat et al. [25] examined the economic index of a one-part GGBFS-based geopolymer binder activated with SH solution at 28 days of compressive strength. Compared to PC with an economic index of $ 2.6/m^3. MPa, geopolymer binder yielded an economic index of $ 2/m^3. MPa, indicating approximately 23% reduction in cost, hence economically viable. From a sustainable viewpoint, assessing GPC is essential due to the environmental and economic crisis globally. However, despite the various studies on the sustainability evaluations of geopolymer concrete, little or no study has been conducted on geopolymer concrete incorporated with GGBFS and CCA, hence, this study.

This study assesses the environmental impacts, sustainability and economic indexes of geopolymer concrete production using the boundary of the cradle-to-site approach [26]. The concrete mix proportions were designed for grade strengths C 30 and 40 MPa and tested for compressive strengths at 28 days. Moreover, the impact factors were acquired from the Inventory of Carbon and Energy (ICE) and relevant works. The findings would assist in instituting the acute variables and circumstances for impact reduction when considering the ecological and financial views of GGBFS-CCA-based GPC production.

2. Materials and methods

2.1. Materials

Corn cobs were obtained and valorized, generating about 30 wt% of corn cob ash (CCA). Granulated blast furnace slag was obtained from the Federated Steel company, Nigeria. The slag was pulverised by an abrasive machine, obtaining GGBFS. Afterwards, the CCA and GGBFS were sieved with 45 µm size to obtain finer particles. Table 1 shows the oxide and physical compositions of binders (CCA, GGBFS, and Portland limestone cement (PLC)) used. The physical properties, such as specific gravity (SG) and specific surface area (SSA), were attained as per BS EN 196–3 [27]. The fineness was examined as per BS EN 196–6 [28]. Fig. 1 indicates the binders' particle size distribution (PSD), investigated by the Laser diffraction, Model Beckman Coulter LS-100. As shown in Table 1, the specific gravity of CCA is lesser than GGBFS and PLC. But, CCA displayed greater fineness and SSA when compared to PLC and GGBFS,

Table 1
Chemical and physical compositions of binders used.

Property	GGBFS	CCA	PLC
CaO, %	36.50	12.65	64.50
SiO_2, %	35.75	62.34	21.55
Al_2O_3, %	14.11	9.55	5.50
Fe_2O_3, %	0.92	10.16	3.08
MgO, %	9.45	1.33	1.52
K_2O, %	0.50	1.15	0.61
Na_2O, %	0.30	0.55	0.14
SO_3, %	1.08	1.30	2.03
TiO_2, %	0.70	0.61	–
P_2O_5, %	0.09	0.20	–
LOI*	1.35	2.95	1.20
SG (g/cm^3)	3.10	2.64	3.15
Fineness (%)	7.6	8.10	7.50
SSA (m^2/kg)	425	515	375

* LOI is the loss of ignition at 850 ^{0}C.

signifying that more volume of CCA and water would be added at partial replacement of GGBFS with CCA [29].

Sharp sand ($\leq$ 4.5 mm size) and granite (12.5–19 mm size) were used as fine and coarse aggregates, respectively. The physical tests on the aggregates showed specific gravities of 2.60 and 2.64 g/cm^3 for fine aggregates (FA) and coarse aggregates (CA), respectively. The moisture contents were 0.70% and 0.80%, while water absorptions were 0.32 and 0.22 for FA and CA. Similarly, aggregates were graded as per BS EN 12620 [30], and the results are shown in Fig. 2. The aggregate samples were obtained and sieved through a set of sieves, and weights retained on each sieve were recorded. After that, the cumulative percentage of weight retained on these set of sieves were summed up.

2.2. Design proportions, preparation, and test

The mix design proportions were performed as per ACI 211.1 [30]. The results are presented in Table 2. The alkaline activators, SH pellets (99% purity) and SS gel were sourced in Agbara, Nigeria. The SS gel consists of Na_2O, SiO_2, and H_2O, having 9.4%, 30.1%, and 60.5%, respectively, with the SiO_2/Na_2O weight ratio of 3.20 and SG of 1.475 g/cm^3 at 20 ^{o}C. Subject to the chemistry procedures by Rajamane and Jeyalakshmi [31] for geopolymer mixes, 354, 400, and 443 g of SH pellets were quantified and dissolved in 646, 600, and 557 g of fresh water to prepare a 12, 14, and 16 M activator, respectively, using SS to SH solutions with a ratio of 2.5:1. The mixing was performed and tested per standard specifications [32–35]. The fresh concrete was placed in the cube in three layers. Each layer received 25 strokes of a 16 mm diameter tamping rod to remove trapped air. After 24 h, the cubes were detached from the moulds and immersed in a water curing tank for 28 days. After 28 days, the cubes were crushed with the aid of a compression machine (Motorised COMTEST 2000 kN) at 3 kN/s of pace.

3. Assessment methodology and data

3.1. Goal and scope

The study evaluates the transport impact (T_i), global warming potential (GWP), global temperature potential (GTP), embodied energy (EE), sustainability index (S_i), and economic index (E_i) of GGBFS-based GPC incorporated with CCA and compares with the conventional concrete. The Kyoto Protocol categorizes greenhouse gasses into six: carbon dioxide (CO_2), methane (CH_4), nitrous oxide (N_2O), hydrofluorocarbons (HFCs), perfluorocarbons (PFCs), and hexafluoride (SF_6) [36]. In the construction and building sector, fossil fuel combustion emits GHG [8,37–40]. Therefore, this study considered CO_2, CH_4, and N_2O as GHG emissions. These emissions are transformed into CO_2 equivalent (CO_2-eq) via the GWP [24,26,38].

3.2. Functional unit and boundary assessment

The functional unit is 1 m^3 of concrete [21,23,41,42]. The concrete's functional unit for embodied energy is set to MJ-eq/m^3. The global warming and global temperature potentials are set to kgCO$_{2-eq}$/m^3. Also, the sustainability and economic indexes are fixed to kgCO$_{2-eq}$/m^3/MPa and \$/m^3/MPa. Furthermore, the investigation was assessed, using cradle-to-site confinement. Fig. 3 shows the boundary for concrete production.

3.3. Inventory data

The ICE and relevant literature were used to obtain the impact factors. The inventory method displays accurate results and great flexibility when used in real case studies [26]. The studies established that waste materials have zero embodied energy and GHG emissions [30,43–47]. Although, corncob has zero EE and GHG emissions at the collection point. Though, the corncob is valorized at a controlled temperature of about 400 °C for 2 h, resulting in energy consumption and GHG emissions. Thus, CCA energy and GHG factors were obtained from the extant literature.
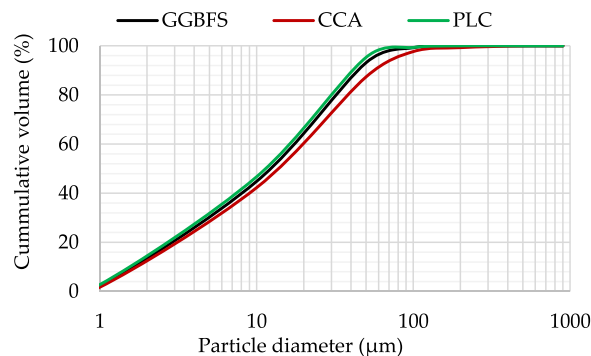

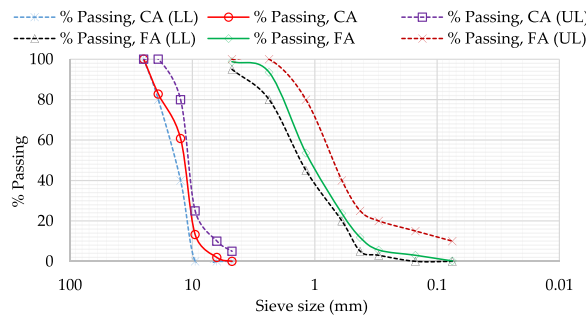**Fig. 1.** The PSD of binding materials used.

Fig. 2. The PSD of aggregates used.

Table 2
Mix design proportions.

| Concrete grade	Mix ID	Binder (kg/m^3)			Aggregate (kg/m^3)		Activator (kg/m^3)		Water (kg/m^3)
		PLC	GGBFS	CCA	FA	CA	SH	SS	
C 30 MPa	A0	380	–	–	734	1045	–	–	205
	A1	–	380	–	899	1045	58.6	146.4	–
	A2	–	304	76	887	1045	58.6	146.4	–
	A3	–	228	152	874	1045	58.6	146.4	–
	A4	–	152	228	865	1045	58.6	146.4	–
	A5	–	76	304	852	1045	58.6	146.4	–
	A6	–	–	380	841	1045	58.6	146.4	–
C 40 MPa	B0	488	–	–	639	1045	–	–	205
	B1	–	488	–	805	1045	58.6	146.4	–
	B2	–	390	98	788	1045	58.6	146.4	–
	B3	–	293	195	772	1045	58.6	146.4	–
	B4	–	195	293	758	1045	58.6	146.4	–
	B5	–	98	390	741	1045	58.6	146.4	–
	B6	–	–	488	728	1045	58.6	146.4	–
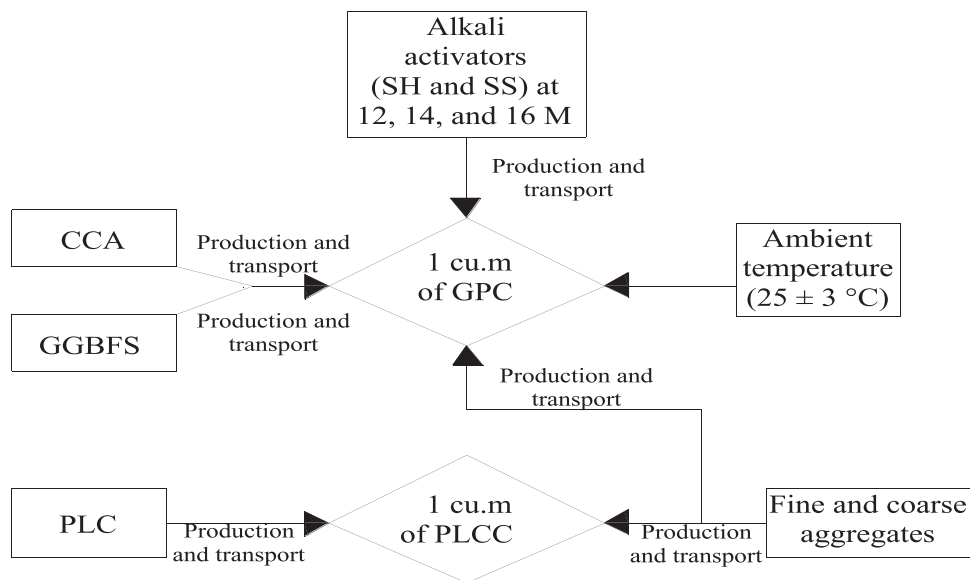
Fig. 3. The boundary for concrete production.

Previous studies established that an elevated curing temperature is required to attain the same mechanical performances of GPC as PCC [48,49]. However, the GPC sample in this study was cured at ambient temperature. Thus, the required energy and GHG emissions for high-temperature curing were disregarded. In addition, no literature reports emissions via the heating of activators under ambient temperature [47]. Furthermore, no superplasticizer was used; hence this assessment does not include admixture energy. Therefore,

Table 3 presents the EE and GWP coefficients (factors). In contrast, Tables 4 and 5 illustrate the GTP and transportation aspects of the concrete ingredients.

3.4. Assessments of environmental impacts

3.4.1. Transportation impact (T_i)

During material transportation, there are fuel energy consumption and greenhouse gas emissions. Thus, Eq. (1) is applied to assess the transportation impacts [21,38,66]. Table 6 shows the details of the distance covered [67].

$$T_i = \sum_{i=1}^{n} \left(m_w \times \frac{d_t \times T_c}{1000} \right) \qquad (1)$$

where m_w = material's weight (kg); d_t = truck distance travelled (km); T_c = transport factors for EE (MJ-eq/tonne-km), GWP (kgCO$_2$-eq/tonne-km), and GTP (kgCO$_2$-eq/tonne-km).

3.4.2. Embodied energy (EE)

The production of 1 m^3 of concrete consumes energy. Hence, Eqs. (2) and (3) are engaged to evaluate the embodied energy of concrete constituents within the cradle-to-site boundary [8,21,26,38].

$$Cradle - to - gate = (1 + m) \sum_{i=1}^{n} (m_w \times EE_c) \qquad (2)$$

$$Cradle - to - site = (1 + m) \sum_{i=1}^{n} (m_w \times EE_c) + TiEE \qquad (3)$$

where m_w = weight of material (kg); m = EE wastage factor (%), taken as 22% [96]; EE_C = EE factors (MJ-eq/kg); TiEE = transport impact of EE (MJ-eq/m^3).

3.4.3. Global warming potential (GWP)

The global warming potential examines the cumulative effect of GHG emissions. This effect comprises short- and long-term gases, altering the mean atmospheric temperature [24]. Thus, Eq. (4) was used to assess the global warming impact of concrete constituents [21,26,38].

$$Cradle - to - site = (1 + n) \sum_{i=1}^{n} (m_w \times GWP_c) + TiGWP \qquad (4)$$

where m_w = weight of material (kg); n = GWP wastage factor (%), taken as 19% [96]; GWP_C = GWP factors (kgCO$_2$-eq/kg); TiGWP = transport impact of GWP (kgCO$_2$-eq/m^3).

3.4.4. Global temperature potential (GTP)

Global temperature potential measures the absolute worldwide temperature change as a result of the GHG emissions during a particular time [24]. Hence, Eq. (5) was used to determine the global temperature impact of concrete constituents [21,26,38].

$$Cradle - to - site = (1 + n) \sum_{i=1}^{n} (m_w \times GTP_c) + TiGTP \qquad (5)$$

where m_w = weight of material (kg); n = GTP wastage factor (%), taken as 19% [96]; GTP_C = GTP factors (kgCO$_2$-eq/kg); TiGTP = transport impact of GTP (kgCO$_2$-eq/m^3).

Table 3
EE and GWP coefficients for concrete constituents.

Constituent	EE$_c$ (MJ-eq/kg)	GWP$_c$ (kgCO$_2$-eq/kg)	Reference
PLC	5.50	95×10^{-2}	[13,24,26,50–54]
GGBFS	1.60	8.3×10^{-3}	[4,26,55,56]
CCA	1.35	8×10^{-3}	[45]
FA	8.1×10^{-2}	5.1×10^{-3}	[4,24,26,47,55,57,58]
CA	8.3×10^{-2}	5.2×10^{-3}	[24,26,47,57,58,59]
SH	18	86×10^{-2}	[56]
SS	5.37	78×10^{-2}	[8,21,38,60,61]
Water	1×10^{-2}	1×10^{-3}	[24,26,62]

Table 4
GTP factors (GTP$_c$).

Constituent	GTP$_c$ (kgCO$_2$-eq/kg)	Reference
PLC	91×10^{-2}	[24,52]
GGBFS	28×10^{-2}	[24]
CCA	9.3×10^{-3}	[24]
FA	4.1×10^{-3}	[24,62]
CA	1×10^{-3}	[24,62]
SH	13×10^{-2}	[63]
SS	73×10^{-2}	[64]
W	4×10^{-4}	[24]

Table 5
Transportation factors (T$_c$) for various types of transportation.

Transportation Mode	Impact Group			Reference
	Energy demand (MJ-eq per tonne-km)	GWP (kgCO$_2$-eq per tonne-km)	GTP (kgCO$_2$-eq per tonne-km)	
Truck, road	2.275	15.9×10^{-2}	16.6×10^{-2}	[8,38,65]
Freight, rail	32.5×10^{-2}	3.9×10^{-2}	–	[8,38,66]
Transoceanic, ship	21.6×10^{-2}	16.5×10^{-2}	–	[8,38,65]

Table 6
Material's transport distance.

Material	Source	Distance (km)	Coordinates
PLC	Ibese	62.0	7.00546, 3.04870
GGBFS	Ota	7.1	6.668667, 3.201111
CCA	Owode-Yewa	17.0	6.71228, 2.97523
FA	Ota	3.5	6.68151, 3.15627
CA	Abeokuta	81.0	7.14761, 3.36195
SH	Lagos	43.8	6.58823, 3.37900
SS	Agbara	25.8	6.579399, 3.088865
Water	Covenant University	0	6.68733, 3.15802

3.5. Sustainability index (S$_i$)

The sustainability index examines the concrete's environmental impacts on the performance of its compressive strength [25,56, 68]. Thus, the index is evaluated per Eq. (6) [69].

$$S_i = \frac{GWP + GTP + \quad (CO_{2i} \times EE)}{f_c} \tag{6}$$

where CO$_{2i}$ is taken as 0.050 kgCO$_2$/MJ [69].

3.6. Economic index (E$_i$)

The economic index assesses the mix feasibility by relating its total cost of production to its compressive strengths [70]. This feasibility is obtained by Eq. (7) [25,67,70].

$$E_i = \frac{C_t}{f_{cu}} \tag{7}$$

where E$_i$ = economic index ($/m^3. MPa); c$_t$ = total cost per a cubic metre of concrete (($/m^3); f$_{cu}$ = compressive strength at 28 days (MPa).

4. Results and discussion

4.1. Compressive strength

As shown in Fig. 4(a) and (b), the results showed a gradual decrease in strength as CCA volume in the mix increased for both grades of concrete. The strength reduction could be the passive reaction of C-S-A-H in the geopolymer paste, retarding the dissolution of CCA

aluminosilicate monomers [15]. Besides, this passive reaction hinders the polycondensation process. This results in an amorphous aluminosilicate product (N-A-S-H) that retards the strength growth [15]. However, a 20–40% replacement of GGBFS with CCA met the 28-day target strength and was higher than control (Portland cement concrete, PCC) for both C 30 and 40 MPa at all concentration levels. Notwithstanding, 14 M yielded the best strength performance compared with 12 and 16 M. Therefore, a maximum of 40% CCA with 60% GGBFS activated GPC can be used as special and reinforced concrete to construct structural elements [35]. A 60–100% replacement of GGBFS with CCA can be used as plain and reinforced concretes for C 30 and 40 concrete grade strengths [35]. It is expedient to state that this investigation merely considered the concrete strengths at 28 days of curing to estimate the sustainability characteristics of GGBFS-CCA-based GPC and compare it with PCC.

4.2. SEM micrographs

As shown in Fig. 5(a), the SEM micrographs revealed an irregular shape with traces of sharp needles. Also, a good interface and adequate compactness were evident due to the chemical reactions between the hydrating agent (calcium-silicate-hydrate) and aggregate quartz, producing a hardened network [15]. As indicated in Fig. 5(b)-(f), the internal microstructures showed amorphous structures in spherical flakes with traces of sharp needles. The chemical reactions between the aluminosilicate monomers in the binders (GGBFS and CCA) and the water glass activating solution results in calcium-aluminate-silicate-hydrate. These results could be responsible for a higher geopolymer concrete strength than PCC [15]. Similarly, Fig. 5(g) reveals spherical flake structures with traces of sharp needles and a good interface. However, the partially unreacted CCA in the matrix could be responsible for the lesser strength than other geopolymer concrete samples [11,15].

4.3. Transportation impact

Fig. 6(a)-(c) present the transport impacts of EE, GWP, and GTP in line with the details outlined in Tables 2, 5, and 6 and Eq. (1). The results revealed that PCC yielded higher EE, GWP, and GTP than GPC. This is because the transportation of PCC constituents per cubic metre is more than GPC constituents, making it longer for PCC mixes than for GPC mixes [67,71]. The total embodied energies, global warming potentials, and global temperature potentials of 252.01 and 266.49 MJ-eq/m^3, 17.61 and 18.63 kgCO$_2$-eq/m^3, and 18.39 and 19.44 kgCO$_2$-eq/m^3 were generated during the transportation of PCC constituents compared with GPC constituents which developed average values of 224.25 and 226.48 MJ-eq/m^3, 15.69 and 15.83 kgCO$_2$-eq/m^3 for C 30 MPa, and 16.37 and 16.53 kgCO$_2$-eq/m^3 for C 40 MPa.

It was also evident from Fig. 6(a)-(c) that transportation impacts of embodied energy, global warming potential, and global temperature potential increased with increasing CCA contents in the GPC mixes for C 30 and 40 MPa. There was approximately 51–80% for the GTP category and 49–80% impact increase of CCA as CCA substitution with GGBFS increased from 20% to 100% for C 30 and C 40, respectively. Similarly, as the percentage replacement of GGBFS with CCA rose from 20% to 100%, there were about 50–80% impact increases in transporting CCA in EE and GWP categories for C 30 and C 40. However, the impact of transporting GGBFS was lower than CCA, mainly because CCA is 58% longer than GGBFS in terms of transport distance. This inference corroborates the findings of Sandanayake et al. [38], where the transport distance for fly ash is 50% longer than cement, demonstrating a significant increase in environmental impact. From Fig. 5(a), about 1–4% and 1–5% contributions of CCA transport impact the GPC's embodied energy as CCA content in the mix increased from 20% to 100% for C 30 and 40 MPa, respectively. Similarly, at 20–100% replacement of GGBFS with CCA, as shown in Fig. 6(b) and (c), the transportation distance impacts of CCA contributed about 1–4% increase in GWP and GTP for C 30 and C 40 MPa.
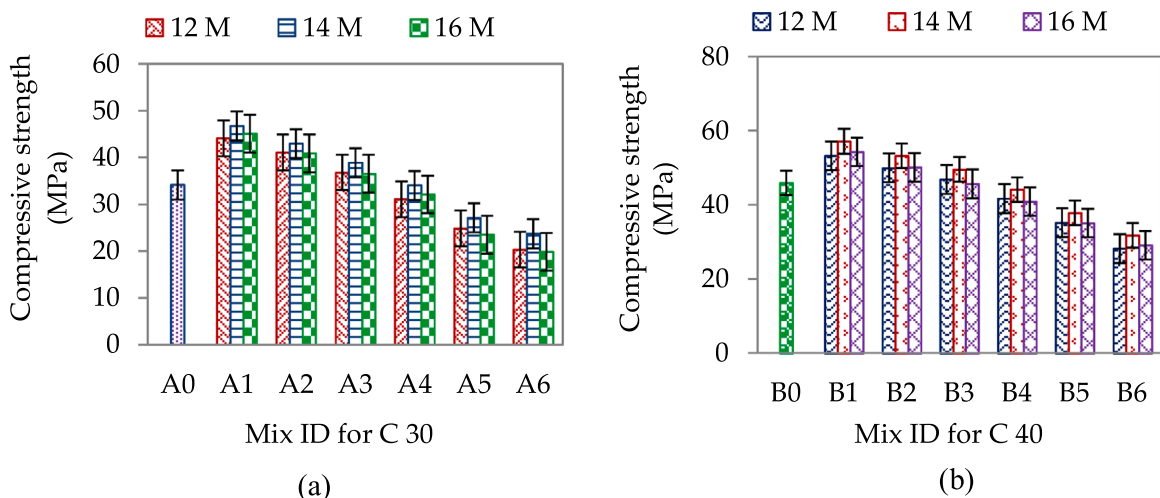

Fig. 4. Compressive strengths at 28 days (a) C 30 MPa and (b) C 40 MPa.
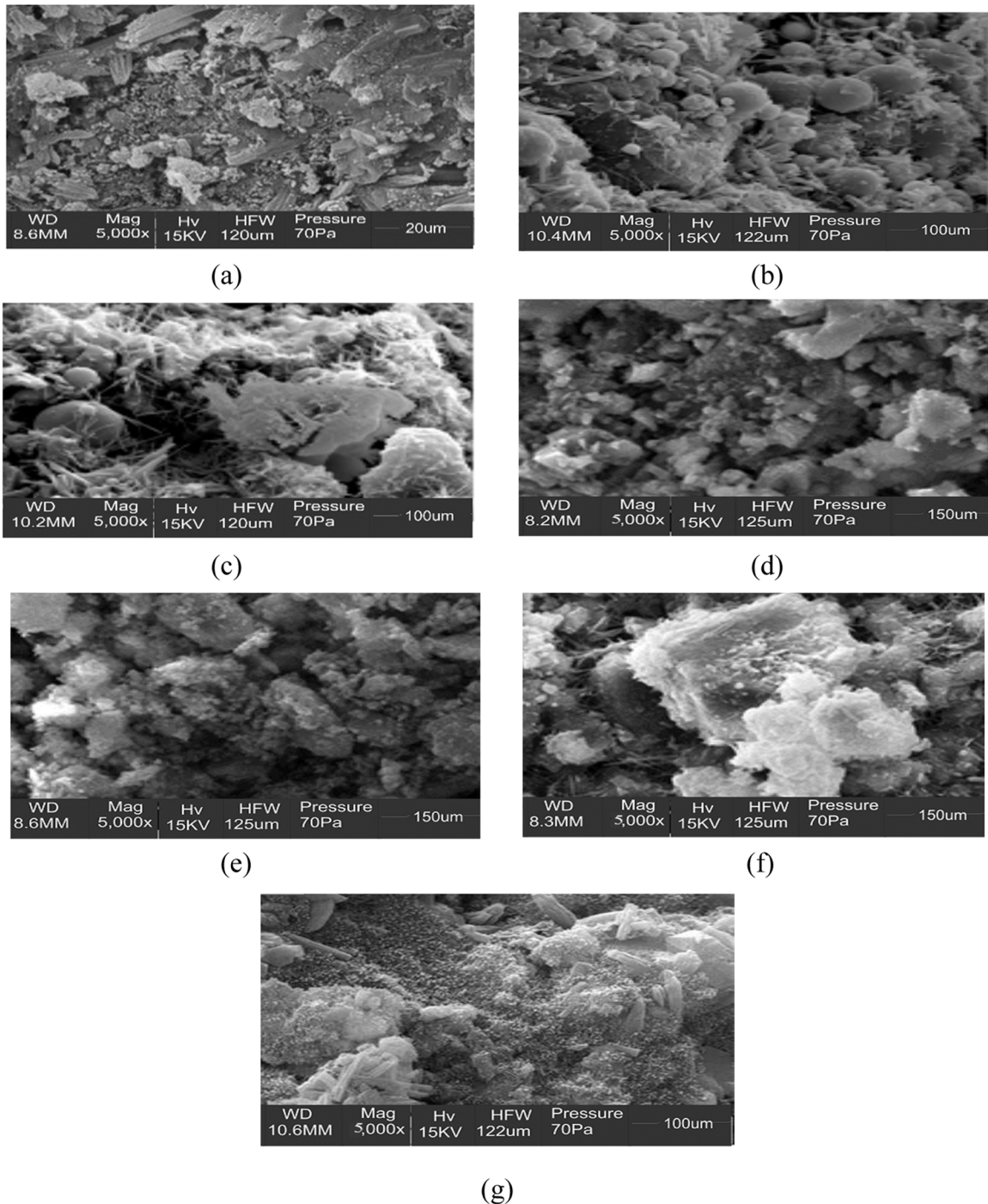
Fig. 5. C 40 MPa SEM micrographs of M 14 activator on (a) 100% PLC (B0), (b) 100% GGBFS (B1), (c) 80% GGBFS + 20% CCA (B2), (d) 60% GGBFS + 40% CCA (B3), (e) 40% GGBFS + 60% CCA (B4), (f) 20% GGBFS + 80% CCA (B5), and (g) 100% CCA (B6).

It can be observed from Fig. 6(a)-(c) that the TiEE, TiGWP, and TiGTP increased as the concrete grade strength increased from 30 to 40 MPa. These can be ascribed to an increase in binding materials (PLC, GGBFS, and CCA) for C 40 mix proportions (B0-B6), representing approximately a 22% increase compared with C 30 grade mix proportions (A0-A6). Above all, transporting concrete constituents interrelates with other concrete components without affecting the concrete's quality [67].
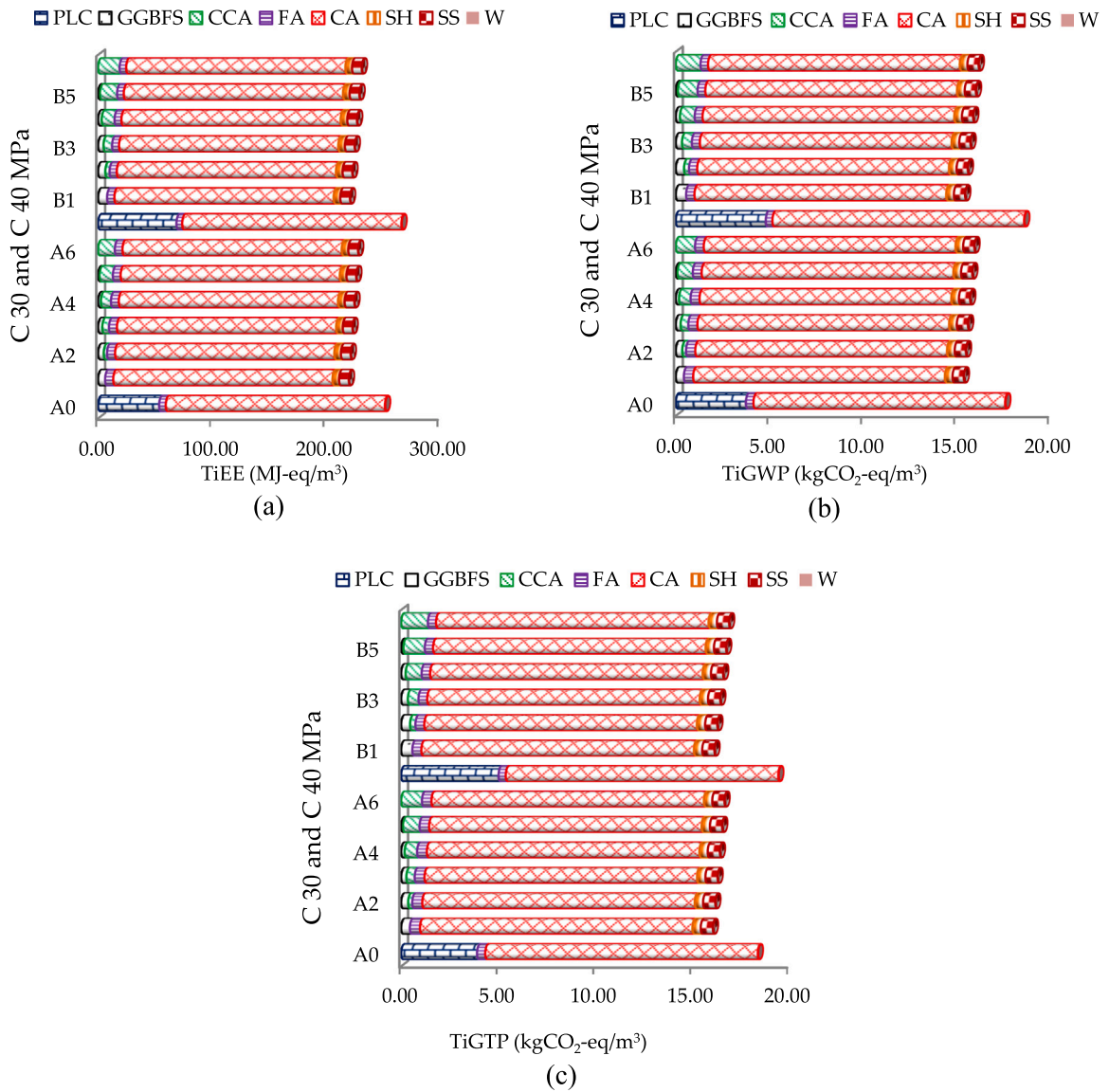
Fig. 6. Transportation impacts (a) embodied energy, (b) global warming potential, and (c) global temperature potential.
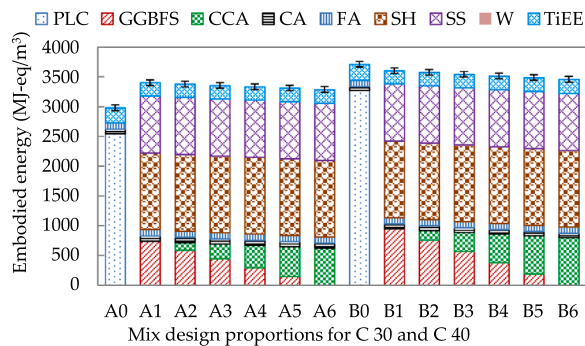

Fig. 7. The EE of GPC and PCC.

4.4. Embodied energy (EE)

Fig. 7 shows the concretes' EE, and the results indicated that GPC exhibited higher EE than PCC for C 30 MPa. The GPC mixes generated about 3289.19–3402.70 MJ-eq/m^3 of EE compared with PCC, which yielded 2982.99 MJ-eq/m^3 of EE. The reasons could be attributed to the statement that the preliminary contribution of constituents for GPC production is higher than PCC. Considering the minimal effect of aggregates on total EE, about 5–7%, the source materials (GGBFS and CCA) and activating solutions (SH and SS) contributed approximately 23.31% and 73.38%, respectively, to the manufacturing of GPC, indicating about 97% of total value compared with PLC which contributed 93.38% to the embodied energy. In the same vein, the water-cement or alkaline liquid-binder ratio was attributed to the earlier stated contribution in that water contributed zero EE to PCC production. In contrast, alkaline liquids (SH and SS) contributed 73.38% of total EE to GPC production, increasing GPC's embodied energy compared with PCC. This aligns with the inferences of Turner and Collins [42], Assi et al. [43], and Alsalman et al. [47] that alkaline activators, SH and SS, are the main contributors to EE of geopolymer products due to the high energy requirements for their production, contributing significant energy variables. However, for concrete grade strength (C 40), GPC yielded lower EE than PCC. There was a 2.89–6.82% reduction in EE of GPC at 0–100% replacement of GGBFS with CCA compared with PCC, where PLC was used as a binder. As shown in Table 2, the reason was due to the water-cement or alkaline liquid-binder (a/b) ratio and binder content. The water-cement (w/c) ratio for C 40 was 0.42 compared with C 30 with a 0.54 w/c ratio, indicating about 23% reduction in water or alkaline liquids' content and a 23% increase in binder's content. Since water contributed zero EE to PCC production, it was evident that PLC, which contributed significant EE to PCC production, contributed 95. 02% for C 40, while GGBFS and CCA used as binders for GPC production contributed 28.15% of EE. Consequently, activating content contributing major EE to GPC production was reduced by approximately 6% compared with C 30, making C 40 exhibit lesser EE than C 30. These results corroborate Alsalman et al.'s [47] findings where about 46% less EE was obtained for GGBFS-fly ash-based GPC activated with SH and SS (C 40 MPa) compared with PCC. The reasons are attributed to OPC utilisation, accounting for about 94–98% of the total OPCC EE; in contrast, fly ash and GGBFS account for about 5% of the total GPC EE. Similarly, Tempest et al. [49] found about 30% less EE in GPC than OPCC for C 60 concrete grade strength. A similar result was affirmed by Assi et al. [43], where the alkali-activated concrete (AAC) yielded an approximately 36% decrease in EE compared with OPCC for C 100 concrete grade strength.

Contrarily, MK-based GPC activated with SH and SS revealed an embodied energy of about 8% higher than OPCC of high-strength concrete grade (C 60 MPa). Metakaolin is not a by-product material; it requires more energy for its production (about 92%) than fly ash and GGBFS production [47]. However, Alsalman et al. [47] suggested that if the energy factor established by Fawer et al. [61] for SS production were used, the embodied energy would have been reduced to 3%.

As shown in Fig. 7, the results signified a decreasing EE as CCA content in GPC mixes increased for all concrete grades because the embodied energy coefficient of CCA is about 16% lesser than GGBFS, indicating CCA is a low EE material [45,72–75]. From Fig. 5, as CCA content in the GPC mixes increased from 0% to 100%, the embodied energy decreased from 3402.70 to 3289.16 MJ-eq/m^3 and 3605.22–3459.15 MJ-eq/m^3 for C 30 (A1-A6) and C 40 (B1-B6), respectively. These reductions signified the EE savings of about 1–4% at 20–100% replacement of GGBFS with CCA for C 30 grade strength. Also, for C 40 grade strength, there was about 1–5% EE saving at 20–100% replacement of GGBFS with CCA. These results align with Abubakar et al.'s [45] findings, where about 3–12% of EE were saved when OPC was replaced with 5–20% of CCA in the blended cement concrete production. Yu et al. [75] reported about 15.6–68. 9% and 0.6–6.8% decrease EE at 25–80% replacement levels of calcined limestone clay and fly ash with OPC, respectively. Besides, about 15.1–66.6% less EE was reported at 25–80% substitution of fly ash in limestone calcined clay-cement-based concrete [75]. Kumar [72] reported a decrease in EE by 25.2% and 29.8% when river sand was replaced with 51% and 100% micro-fine stone sludge (MFSS) to produce structural grade cellular concrete. In the same vein, Patil et al. [74] discovered a 16% reduction in EE when OPC was replaced with 50% natural pozzolanic volcanic ash. These findings demonstrate the attainment of energy-lessening GGBFS-CCA-based GPC to compete favourably with the PCC.
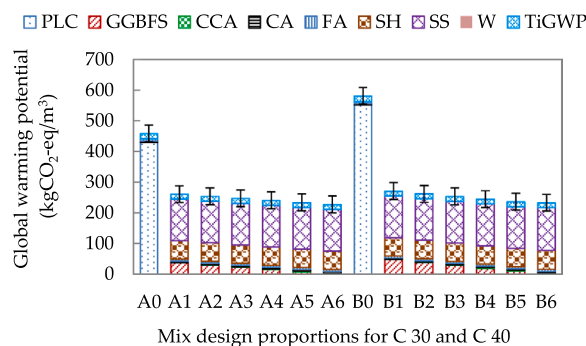

Fig. 8. GWP of GPC and PCC.

4.5. Global warming potential (GWP)

As shown in Fig. 8, the results signified a lesser GWP in GPC than PCC for all concrete mixes. This is because the environmental impact of PLC contributes 93.73% and 94.98% and generates 458.33 and 580.85 kgCO$_2$-eq /m^3 for C 30 and 40 MPa. However, during the extraction of natural pozzolan/GGBFS, only 0.000093 kgCO$_2$-eq/m^3 is generated with 100 ^{o}C maximum temperature required for the conditioning process (drying, grinding, and homogenisation) [24]. The total GWP in GPC mixes varied from 227 to 261 kgCO$_2$-eq/m^3 associated with PCC, which generated approximately 459 kgCO$_2$-eq/m^3 of GWP for C 30 concrete grade strength. In the same, C 40 grade strength exhibited about 233–271 kgCO$_2$-eq/m^3 for GPC mixes, while PCC mix yielded approximately 581 kgCO$_2$-eq/m^3 of total GWP. In this respect, Robayo-Salazar et al. [24] described a 44.7% less GWP in natural volcanic pozzolan-GGBFS-based GPC activated with SH and SS than PCC. Similarly, Habert et al. [23] stated that fly ash-based GPC yielded approximately 45% lesser GWP than PCC. Mclellan et al. [21] and Heath et al. [22] also affirmed the feasible reduction in GWP by 40–44% with geopolymer innovation in place of PLC based on the cradle-to-site approach. In addition, Dal Pozzo et al. [76] reported about 42% lesser GWP for fly ash-based GPC than PCC. Compared with PCC, Heath et al. [22] found about 40% less GWP for MK, bentonite meta-clay, and SF-based GPC activated with 50% and 37% solids of both SH and SS, respectively. Also, Sandanayake et al. [38] reported a 5–10% decrease in GWP of fly ash-based GPC activated with 15 M of SH and SS compared with PCC. Regardless of these associated studies, Fernando et al. [8] observed a conflicting outcome where fly ash-RHA- based GPC activated with 15 M of SH and SS yielded approximately 12% increment in GWP than PCC due to heat curing requirement to achieve strength development, contributing about 9% to the total GWP.

As indicated in Fig. 8, the aggregates (FA and CA) yielded low GWP results both in PCC and GPC; these constituents contributed less than 5% to the total GWP of the concrete production process. Considering the binders, approximately 1–2% of GWP was responsible for CCA at all levels of concrete grade strengths. Besides, GGBFS contributed about 4–15% and 4–18% of GWP to the total GWP for C 30 and 40 MPa, respectively. In contrast, 94% and 95% of total GWP were responsible for PLC production in C 30 and 40 MPa. These findings align with the relevant investigations where fly ash, GGBFS, and PLC contributed about 1%, 16%, and 95% to the total GWP, respectively [8,23,24,77]. On the other hand, the alkaline activators (SH and SS), as shown in Fig. 7, contributed about 22–27% and 50–60%, respectively, to the total GWP for both C 30 and 40 MPa. These support the outcomes of Fernando et al. [8], where SS caused around 52% of the total GWP. Moreover, SH and SS contributed approximately 74% to the total GWP. This corroborates with Heath et al. [22], which reported that SS contributed 44–59% to GWP. Moreover, the relevant study aligns with these results in that SH and SS used in natural volcanic pozzolan-GGBFS GPC contributed 18.89% and 66.35%, respectively, totalling 85.24% the total GWP [24].

It is essential to state that GWP is reduced as CCA content in the GPC mixes increases. At 20–100% replacement of GGBFS with CCA content in the GPC mix, there was about 3–13% saving in total GWP for C 30 and 40 MPa. This indicates CCA is a low GWP exhibitor. This assertion follows the findings of Abubakar et al. [45], where about 4–17% of GHG emissions were saved when OPC was replaced by 5–20% of CCA in the blended cement concrete production.

From Fig. 8, it was evident that GWP increased upon increasing concrete grade due to the decreasing water-cement ratio with increasing concrete grade. Hence, the contribution of binder content (PLC for PCC production) on one hand or the SCMs (GGBFS and CCA contents for GPC production) on the other hand to the total GWP increased, thereby making C 40 exhibit higher GWP than C 30. As observed in the PCC mix, there was 21.09% higher GWP in C 40 than in C 30 grade strength. Similarly, GPC mixes generated about 3–4% higher GWP for C 40 than C 30 grade strength. Nonetheless, GPC incorporates exhibited lesser GWP than the PCC mix. These corroborate the findings of Bianco et al. [41], where the GWP of PCC and fly ash-GGBFS-based GPC activated with commercial SH-SS showed 333 and 123 kgCO$_2$-eq/m^3 for C 35, 409 and 142 kgCO$_2$-eq/m^3 for C 50, and 507 and 181 kgCO$_2$-eq/m^3 for C 70, respectively. These signified about 65% increase in GWP for PCC compared with fly ash-GGBFS-based GPC for C 35, 40, and 70 MPa. Therefore, mitigating the global warming impact of PLC production requires alternatives such as GGBFS and CCA, driving a cleaner environment and sustainable product [78–80].
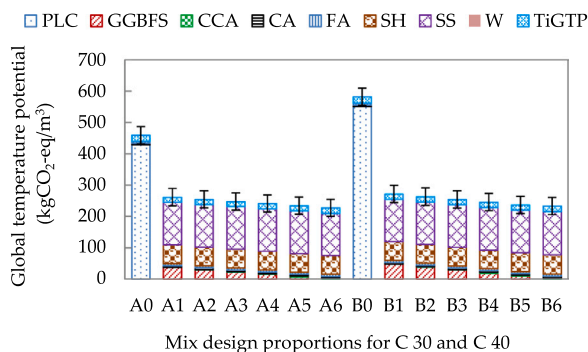

Fig. 9. Global temperature potentials of GPC and PCC.

4.6. Global temperature potential (GTP)

Fig. 9 shows the results of global temperature potentials. The PCC generated higher GTP than GPC at all concrete mixes due to the high temperature needed for the PLC clinkerization process (1350–1450 ^{o}C). In contrast, CCA only requires a temperature of about 400 ^{o}C for its valorisation, while alkaline activators are obtained at low temperatures of about 25–100 ^{o}C. In addition, GGBFS is an industrial waste product without carbon dioxide, methane, and other related gases. This affirms Robayo-Salazar et al.'s [24] findings that concrete constituents' impact GTP: PLC for PCC production, or precursor for GPC production, and the alkaline proportions. As shown in Fig. 8, the total GTP in PCC showed 435.96 and 533.86 kgCO$_2$-eq/m^3 for C 30 and C 40 MPa, compared with the total GWP in GPC, which varied from 285.10 to 163.22 kgCO$_2$-eq/m^3 and 321.05–164.50 kgCO$_2$-eq/m^3 for C 30 and 40 MPa. These results align with Robayo-Salazar et al. [24], which found about a 47% increase in GTP for PCC compared with GPC.

As highlighted in Fig. 8 for GWP, the aggregates (FA and CA) and GPC precursors (CCA and GGBFS) contributed minimal impacts to the overall GTP of the concretes. Aggregates, CCA, and GGBFS contributed about 1–2%, 1–3%, and 4–15%. On the other hand, the alkaline activators SH and SS contributed about 19–37% and 42–85% to the total GPC GWP for C 30 and 40 MPa. These corroborate the results of Robayo-Salazar et al. [24], which found that SS and SH were responsible for 66.35% and 18.89% of the total GWP for natural volcanic pozzolan-GGBFS-based GPC, respectively; and the contribution rate of SH and SS was accounted for 85.24% of the total GWP.

At 20–100% replacement of GGBFS with CCA for GPC mixes, 8.55–42.75% of GTP were saved for C 30 MPa strength grade. Similarly, C 40 MPa saved 9.79–48.76% of GWP when GGBFS was replaced by CCA at 20–100%, respectively. These findings infer that GGBFS-CCA-based GPC is a greener concrete, demonstrating an environmentally sustainable product that can be utilised in the construction industry.

4.7. Sustainability index (S$_i$)

Fig. 10 indicates the sustainability index for GPC and PCC. The results revealed that PCC exhibited a higher S$_i$ than GPC, signifying that GPC is highly sustainable than PCC [56,69]. Compared to PCC, with a sustainability index of 30.55 kgCO$_2$-eq/m^3 MPa, the sustainability index for GPC, yielded about 15–28 kgCO$_2$-eq/MPa per cubic metre of GPC for C 30 MPa. Similarly, for C 40 MPa, the sustainability index of GPC was 14–20 kgCO$_2$-eq/MPa/m^3, compared with the PCC, having approximately 29 kgCO$_2$-eq/MPa/m^3. The reasons could not be far-fetched: GPC yielded higher compressive strength and lesser environmental impacts than PCC. These results support the findings reported by Adesina [56], where slag-based GPC activated with SS and SH exhibited about 57% lesser sustainability index than PCC. In addition, relevant studies reported sustainable concrete incorporated with GGBFS, fly ash, and SF [81–84].

As shown in Fig. 10, it is pertinent to state that 14 M exhibited the lowest sustainability index compared with 12 and 16 M, indicating that 14 M is more sustainable than 12 and 16 M for both C 30 and 40 MPa. At 0–100 wt% replacements of GGBFS with CCA for C 30 MPa, 12 M showed a higher sustainability index of 5.59–14.41% than 14 M. Also, I6 M exhibited a 6.78–11.26% higher sustainability index than 14 M, while 16 M yielded a 4.90–8.46% higher sustainability index than 14 M at 0–100 wt% replacements of GGBFS with CCA for C 40 MPa. These results are associated with the highest compressive strength obtained for 14 M instead of 12 and 16 M. In addition, 14 M of SH activation with SS is recommended, demonstrating the highest compressive strength and the lowest sustainability index. In addition, a 60–100 wt% of CCA substitution satisfied the mass concreting strength requirements [35]. Thus, it is sustainable for non-load bearing applications.

4.8. Economic index (Ei)

Table 7 shows the costs of materials used for the assessment. The costs include materials, material processing, and transportation. Similarly, the total cost per concrete cubic metre is shown in Table 8.

As shown in Table 8, PCC yielded a minimal cost reduction of about 112 and 134 $/m^3 compared with GPC, which varied from 127 to 131 $/m^3 and 133–139 $/m^3 for C 30 and 40 MPa. This performance is primarily owing to the purchasing cost of alkali activators (SH and SS), which is about 73% higher than PLC. At 0–100 GGBFS wt% replacement, there were about 11.82–14.71% and 0–4%
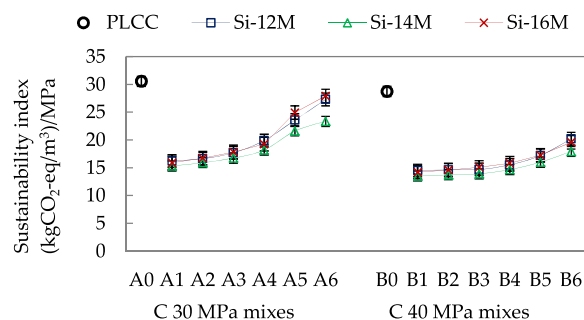

Fig. 10. S$_i$ of GPC and PCC.

Table 7

Material costs ($/kg).

Material	Processing	Material	Transportation	Total
PLC	–	0.200	0.0097	0.210
GGBFS	0.075	–	0.005	0.080
CCA	0.065	–	0.005	0.070
FA	–	0.0085	–	0.0085
CA	–	0.024	–	0.024
SH pellets	–	0.500	0.0090	0.509
SS gel	–	0.250	0.0090	0.259
Water	–	0.0024	–	0.0024

Table 8

The total cost per 1 m^3 of concrete.

Concrete grade	Mix ID	PLC	GGBFS	CCA	FA	CA	SH	SS	W	Total cost ($/$m^3$)
C 30 MPa	A0	79.80	-	-	6.24	25.08	-	-	0.49	111.61
	A1	-	30.40	-	7.64	25.08	29.83	37.92	-	130.87
	A2	-	24.32	5.32	7.54	25.08	29.83	37.92	-	130.01
	A3	-	18.24	10.64	7.43	25.08	29.83	37.92	-	129.13
	A4	-	12.16	15.96	7.35	25.08	29.83	37.92	-	128.30
	A5	-	6.08	21.28	7.24	25.08	29.83	37.92	-	127.43
	A6	-	-	26.60	7.15	25.08	29.83	37.92	-	126.57
C 40 MPa	B0	102.48	-	-	5.43	25.08	-	-	0.49	133.48
	B1	-	39.04	-	6.84	25.08	29.83	37.92	-	138.71
	B2	-	31.20	6.86	6.70	25.08	29.83	37.92	-	137.58
	B3	-	23.44	13.65	6.56	25.08	29.83	37.92	-	136.48
	B4	-	15.60	20.51	6.44	25.08	29.83	37.92	-	135.38
	B5	-	7.84	27.30	6.30	25.08	29.83	37.92	-	134.26
	B6	-	-	34.16	6.19	25.08	29.83	37.92	-	133.17

higher production costs in GPC than PCC for C 30 and 40 MPa. These results affirm Mclellan et al. [21] findings, where the production costs of C 40 MPa strength grade of fly ash-SF-based GPC activated with SH, fly ash-based GPC activated with SH and SS, and fly ash-SF-gibbsite-based GPC activated with SH were 21%, 11%, and 39% higher than OPCC. In addition, Fernando et al. [8] reported a similar finding where about $ 86 cost reduction was obtained for PCC production compared with GPC of the same strength grade. A contrary study reported that the costs of producing fly ash-based GPC activated with SH and SS, fly ash-SF-based GPC activated with SH and SS, and fly ash-SF-based GPC activated with SH were 10.87%, 11.52%, and 17.77% lesser than PCC [67]. Notwithstanding, for further study, sodium carbonate may be used to replace SH and SS used in this study to reduce the higher cost arising from the GPC production compared with PCC. It has been established that sodium carbonate as an activator in alkali-activated concrete is more economical, accounting for 33.33% less SH and SS [85]. Also, sodium carbonate is more environmentally friendly than SH and SS [56].

From Table 8, PLC contributed approximately 72% and 77% to the entire budget of producing PCC in comparison with precursors (GGBFS and CCA), which contributed about 21–23% and 26–28% to the entire budget of GPC production for C 30 and 40 MPa. Moreover, the total costs of about 52–54% and 49–51% were contributed by the alkali activators (SH and SS) to GPC production. These results align with Fernando et al.'s [8] findings, where PLC and alkali activators (SH and SS) were responsible for 74% and 53% of initial costs for PCC and GPC productions, respectively. In addition, incorporating CCA in the GPC mixes resulted in a cost reduction compared with GGBFS. There was about a 2–10% total cost reduction in producing GPC at 20–100 wt% of CCA substitution for both C 30 and 40 MPa. This also supports the findings of Fernando et al. [8], where a partial replacement of fly ash with 10 wt% of RHA reduced the total cost of producing GPC/m^3 by 3%. Nonetheless, change is constant, signifying that the cost of concrete constituent changes owing to the geographical scenario and processing and transportation types [8]. Using the relationship illustrated in Eq. (7), Fig. 11 displays the concrete's economic index.

Fig. 11 shows that GPC, at 40 wt% optimum replacement of GGBFS with CCA exhibits a lesser economic index than PCC at both C 30 and 40 MPa, indicating GPC is an economically efficient concrete [25,68,70,86]. Compared with 3.27 $/$m^3$MPa for PCC, there was about 2.80 lower up to 6.37 higher economic index in GPC for C 30 MPa. Similarly, there was about 2.43 lower up to 4.72 higher economic indexes in GPC than PCC, with the economic index of 2.90 3.27 $/$m^3$. MPa for C 30 MPa.

As indicated in Fig. 11, C 40 MPa showed higher economic efficiency than C 30 MPa for GPC and PCC. This performance could be related to the fact that C 40 MPa yielded a higher strength than C 30 MPa. On the other hand, 14 M activation exhibited the lowest economic index compared with 12 and 16 M activations in GPC mixes. At 0–100 wt% CCA substitution, 14 M yielded approximately 6–14% and 7–11% lesser economic index than 12 M for C 30 and 40 MPa. In the same vein, 14 M exhibited about 4–13% and 5–9% lesser economic index than 16 M for C 30 and 40 MPa. As a result of these findings, the economic prospects of GGBFS-CCA-based-GPC can only be attainable at a 40 wt% optimum replacement of GGBFS with CCA using the 14 M activation.
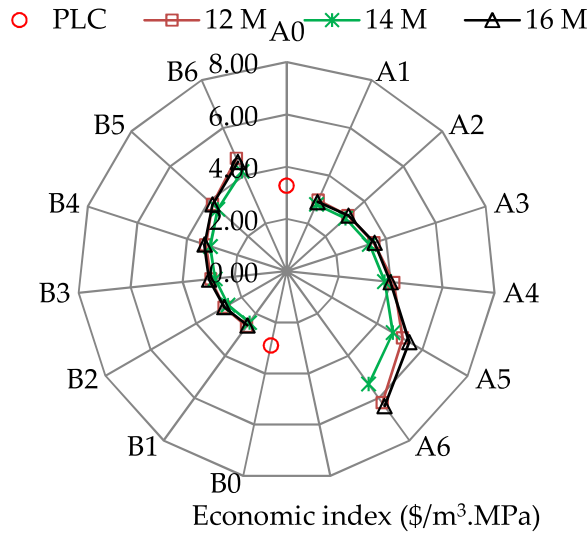
Fig. 11. Economic index of GPC and PCC.

4.9. Model equation between GTP and GWP

As shown in Fig. 12, the linear relationship between GTP and GWP of GPC yielded a strong correlation with 98.87% R^2. Little or no study on this relationship hampers the model validation.

5. Conclusions

This study evaluated the sustainability of slag-based GPC incorporated with CCA. The environmental impact factors were sourced from ICE using the cradle-to-site boundary. Moreover, the sustainability and economic indexes of the concrete were evaluated. Hence, the following conclusions are made:

   i. In comparison to PCC mix, the total EE of GPC mixes increased by 9–12% for C 30 MPa.
   ii. For C 40 MPa, geopolymer mixtures show EE that is 3–7% lower than the PCC mix.
   iii. Regarding overall GWP, GPC mixes saved between 43% and 51% and 54% and 60% when compared to PCC mixes for C 30 and 40 MPa, respectively.
   iv. When GPC C 30 and 40 MPa were produced, as opposed to PCC manufacturing, corresponding global temperature potentials of around 35–63% and 42–70% were preserved.
   v. For C 30 and C 40 MPa, geopolymer concrete is approximately 11–50% and 30–52% more sustainable than PCC.
   vi. At a 40% substitution of GGBFS with CCA, the economic efficiency of GPC was better than PCC.

This study offers viable prospects for GGBFS-CCA-based GPC in reducing the environmental impacts of PCC production. Also, it provides an emerging potential for sustainable and economic efficiency. The study's outcomes will aid the researchers to achieve a
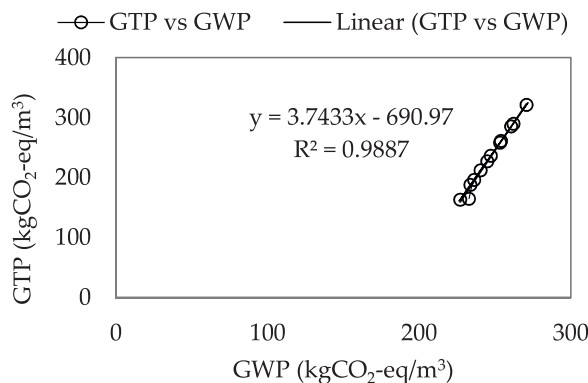

Fig. 12. Relationship between GTP and GWP of GPC.

cleaner environment and sustainable production in the construction division. Despite these promising findings, additional research with other alkaline activators (user-friendly) should be looked at to determine their environmental effects on the production of GGBFS-CCA-Based GPC.

Declaration of Competing Interest

The authors declare that they have no known competing financial interests or personal relationships that could have appeared to influence the work reported in this paper.

Data availability

Data will be made available on request.

Acknowledgements

References

[1] P. Bun, M. Cyr, P. Laniesse, K.N. Bun, R. Idir, Concrete made of 100% recycled materials - a feasibility study, Res. Conserv. Recycl. 180 (2022), 106199, https://doi.org/10.1016/j.resconrec.2022.106199.

[2] Md.H. Uzzal, L. Jin-Cheng, X. Dongxing, Ng Thomas, Y. Hailong, J.A. Safaa, Designing sustainable concrete mixes with potentially alternative binder systems: multicriteria decision making process, J. Build. Eng. 45 (2022), 103587, https://doi.org/10.1016/j.jobe.2021.103587.

[3] T.G. Jerome, J.D. Ithan, B.B. Arnel, R.T. Raymond, B.P. Michael, Life cycle assessment of self-healing geopolymer concrete, Clean. Eng. Technol. 4 (2021), 100147, https://doi.org/10.1016/j.clet.2021.100147.

[4] P. Kathirvel, S. Sreekumaran, Sustainable development of ultra-high-performance concrete using geopolymer technology, J. Build. Eng. 39 (2021), 102267, https://doi.org/10.1016/j.jobe.2021.102267.

[5] R.M. Andrew, Global CO$_2$ emissions from cement production, Earth Syst. Sci. Data 11 (2019) 1675–1710, https://doi.org/10.5194/essd-11-1675-2019.

[6] E. Thwe, D. Khatiwada, A. Gasparatos, Life cycle assessment of a cement plant in Naypyitaw, Myanmar, Clean. Environ. Syst. 2 (2021), 100007, https://doi.org/10.1016/j.cesys.2020.100007.

[7] O.F.A. Perez, D.R. Florez, L.M.Z. Vergara, K.V.H. Benavides, Innovative use of agro-waste cane bagasse ash and waste glass as cement replacement for green concrete. Cost analysis and carbon dioxide emissions, J. Clean. Prod. 379 (2022), 134822, https://doi.org/10.1016/j.jclepro.2022.134822.

[8] S. Fernando, C. Gunasekara, D.W. Law, M.C.M. Nasvi, S. Setunge, R. Dissanayake, Life cycle assessment and cost analysis of fly ash-rice husk ash blended alkali-activated concrete, J. Environ. Manag. 295 (2021), 113140, https://doi.org/10.1016/j.jenvman.2021.113140.

[9] M.S. Imbabi, C. Carrigan, S. McKenna, Trends and developments in green cement and concrete technology, Int. J. Sustain. Built Environ. 1 (2012) 194–216, https://doi.org/10.1016/j.ijsbe.2013.05.001.

[10] S.K. Nath, N.S. Randhawa, S. Kumar, A review on characteristics of silicomanganese slag and its utilization into construction materials, Res. Conserv. Recycl. 176 (2022), 105946, https://doi.org/10.1016/j.resconrec.2021.105946.

[11] E. Aprianti, P. Shafigh, S. Bahri, J.N. Farahani, Supplementary cementitious materials origin from agricultural wastes: a review, Constr. Build. Mater. 74 (2015) 176–187, https://doi.org/10.1016/j.conbuildmat.2014.10.010.

[12] G.C. Isaia, High-performance concrete for sustainable constructions, Waste Mater. Constr. 15 (2000) 344–354, https://doi.org/10.1016/S0713-2743(00)80047-1.

[13] D.J.M. Flower, J.G. Sanjayan, Greenhouse gases emissions due to concrete manufacture, Int. J. Life Cycle Assess. 12 (2007) 282, https://doi.org/10.1065/lca2007.05.327.

[14] A. Mehta, R. Siddique, Sustainable geopolymer concrete using ground granulated blast furnace slag and rice husk ash: Strength and permeability properties, J. Clean. Prod. 205 (2018) 49–57, https://doi.org/10.1016/j.jclepro.2018.08.313.

[15] S. Oyebisi, A. Ede, F. Olutoge, D. Omole, Geopolymer concrete incorporating agro-industrial wastes: effects on mechanical properties, microstructural behaviour and mineralogical phases, Constr. Build. Mater. 256 (2020), 119390, https://doi.org/10.1016/j.conbuildmat.2020.119390.

[16] S. Oyebisi, A. Ede, F. Olutoge, S. Ogbiye, Evaluation of reactivity indexes and durability properties of slag-based geopolymer concrete incorporating corn cob ash, Constr. Build. Mater. 258 (2020), 119604, https://doi.org/10.1016/j.conbuildmat.2020.119604.

[17] S.E. Wallah, Sulfate and acid resistance of fly ash-based geopolymer concrete, : Aust. Struct. Eng. Conf. Eng., Aust. (2005).

[18] J.M. Paris, J.G. Roessler, C.C. Ferraro, H.D. DeFord, T.G. Townsend, A review of waste products utilized as supplements to Portland cement in concrete, J. Clean. Prod. (2015), https://doi.org/10.1016/j.jclepro.2016.02.013.

[19] B.L. Damineli, F.M. Kemeid, P.S. Aguiar, V.M. John, Measuring the eco-efficiency of cement use, Cem. Concr. Compos. 32 (2010) 555–562, https://doi.org/10.1016/j.cemconcomp.2010.07.009.

[20] Food and Agriculture Organization of the United Nations, Food and Agriculture Organization Statistical Pocketbook World Food and Agriculture (FAOSTAT Data); Food and Agriculture Organization of the United Nations: Rome, Italy, 2017.

[21] B.C. Mclellan, R.P. Williams, J. Lay, A. Van Riessen, G.D. Corder, Costs and carbon emissions for geopolymer pastes compared to ordinary Portland cement, J. Clean. Prod. 19 (2011) 1080–1090, https://doi.org/10.1016/j.jclepro.2011.02.010.

[22] A. Heath, K. Paine, M. Mcmanus, Minimizing the global warming potential of clay-based geopolymers, J. Clean. Prod. 78 (2014) 75–83, https://doi.org/10.1016/j.jclepro.2014.04.046.

[23] G. Habert, C. Ouellet-Plamondon, Recent update on the environmental impact of geopolymers, RILEM Tech. Lett. 1 (2016) 17–23.

[24] R. Robayo-Salazar, J. Mejía-Arcila, R.M. De Gutierrez, E. Martínez, Life cycle assessment (LCA) of an alkali-activated binary concrete based on natural volcanic pozzolan: a comparative analysis to OPC concrete, Constr. Build. Mater. 176 (2018) 103–111, https://doi.org/10.1016/j.conbuildmat.2018.05.017.

[25] M. Refaat, A. Mohsen, E.A.R. Nasr, M. Kohail, Minimizing energy consumption to produce safe one-part alkali-activated materials, J. Clean. Prod. 323 (2021), 129137, https://doi.org/10.1016/j.jclepro.2021.129137.

[26] G.P. Hammond, C.I. Jones, Inventory of (embodied) Carbon & Energy Database (ICE), Version 2.0 (Ed. F. Lowrie, and P. Tse)," University of Bath, United Kingdom, 2011. Available at: ⟨https://greenbuildingencyclopaedia.uk/wp-content/uploads/2014/07/Full-BSRIA-ICE-guide.pdf⟩.

[27] British Standard EN 196- 3, Method of Testing Cement: Physical Test, BSI, London, 2016.

[28] British Standard EN 196–6, Methods of Testing Cement: Determination of Fineness, BSI, London, 2018.

[29] S.U. Khan, M.F. Nuruddin, T. Ayub, N. Shafiq, Effects of different mineral admixtures on fresh concrete properties, Sci. World J. 986567 (2014) 1–11, https://doi.org/10.1155/2014/986567.

[30] American Concrete Institute 211.1, Standard Practice for Selecting Proportions for Normal, Heavyweight, and Mass Concrete: ACI, Farmington Hills, USA, 2002.

[31] N.P. Rajamane, R. Jeyalakshmi, Quantities of Sodium Hydroxide Solids and Water to prepare Sodium Hydroxide Solution of given Molarity for Geopolymer Concrete Mixes, Indian Concrete Institute Technical Paper, SRM Univ., India (2014).

[32] British Standard 1881–125, Testing Concrete: Methods for Mixing and Sampling Fresh Concrete in the Laboratory, BSI, London, 2013.

[33] British Standard EN 12390–2, Testing Hardened Concrete: Making and Curing for Strength Tests, BSI, London, 2019.

[34] British Standard EN 12390- 3, Testing Hardened Concrete: Compressive Strength of Test Specimens, BSI, London, 2009.

[35] British Standard EN 206, Concrete Specifications, Performance, Production and Conformity. BSI, London, 2016.

[36] H. Iwata, K. Okada, Greenhouse gas emissions and the role of the Kyoto Protocol, Environ. Econ. Pol. Stud. 16 (4) (2014) 325–342. ⟨https://mpra.ub.uni-muenchen.de/22299/⟩.

[37] M. Sandanayake, G. Zhang, S. Setunge, W. Luo, C.Q. Li, Estimation and comparison of environmental emissions and impacts at foundation and structure construction stages of a building a case study, J. Clean. Prod. 151 (2017) 319–329, https://doi.org/10.1016%2Fj.jclepro.2017.03.041.

[38] M. Sandanayake, C. Gunasekara, D. Law, G. Zhang, S. Setunge, Greenhouse gas emissions of different fly ash-based geopolymer concrete in building construction, J. Clean. Prod. 204 (2018) 399–408, https://doi.org/10.1016/j.jclepro.2018.08.311.

[39] H. Yan, Q. Shen, L.C.H. Fan, Y. Wang, L. Zhang, Greenhouse gas emissions in building construction: a case study of one Peking in Hong Kong, Build. Environ. 45 (4) (2010) 949–955, https://doi.org/10.1016/j.buildenv.2009.09.014.

[40] G. Zhang, M. Sandanayake, S. Setunge, C. Li, J. Fang, Selection of emission factor standards for estimating emissions from diesel construction equipment in building construction in the Australian context, J. Environ. Manag. (2017), https://doi.org/10.1016/j.jenvman.2016.10.068.

[41] L. Bianco, B.D. Tomos, R. Vinai, Analysis of the environmental impacts of alkali-activated concrete produced with waste glass-derived silicate activator - a LCA study, J. Clean. Prod. 316 (2021), 128383, https://doi.org/10.1016/j.jclepro.2021.128383.

[42] L.K. Turner, F.G. Collins, Carbon dioxide equivalent (CO_2-e) emissions: a comparison between geopolymer and OPC cement concrete, Constr. Build. Mater. 43 (2013) 125–130, https://doi.org/10.1016/j.conbuildmat.2013.01.023.

[43] L. Assi, K. Carter, E. Deaver, A.R. Eddie, P. Ziehl, Sustainable concrete: building a greener future, J. Clean. Prod. 198 (2018) 1641–1651, https://doi.org/10.1016/j.jclepro.2018.07.123.

[44] T. Stengel, D. Heinz, J. Reger, Life cycle assessment of geopolymer concrete-what is the environmental benefit, Proc. 24th Bienn. Conf. Concr. Inst. Aust. (2009) 54–62.

[45] A. Abubakar, A. Mohammed, D. Samson, Assessment of embodied energy and CO_2 emission of concrete containing corncob ash, Int. J. Sustain. Green. Energy 10 (2) (2021) 76–84. ⟨http://www.sciencepublishinggroup.com/j/ijsge⟩.

[46] B. Tempest, O. Sanusi, J. Gergely, V. Ogunro, D. Weggel, Compressive strength and embodied energy optimization of fly ash-based geopolymer concrete, World Coal Ash (WOCA) Conf. (2009) 1–17.

[47] A. Alsalman, L.N. Assi, R.S. Kareem, K. Carter, P. Ziehl, Energy and CO_2 emission assessments of alkali-activated concrete and Ordinary Portland Cement concrete: a comparative analysis of different grades of concrete, Clean. Environ. Syst. 3 (2021), 100047, https://doi.org/10.1016/j.cesys.2021.100047.

[48] P. Duxson, A. Fernandez-Jimenez, J.L. Provis, G.C. Lukey, A. Palomo, J.S.J. van Deventer, Geopolymer technology: the current state of the art, J. Mater. Sci. 42 2917–2933. https://doi.org/10.1007/s10853–006-0637-z.

[49] A. Palomo, M.W. Grutzeck, M.T. Blanco, Alkali-activated fly ashes: a cement for the future, Cem. Concr. Res 29 (1999) 1323–1329, https://doi.org/10.1016/S0008-8846(98)00243-9.

[50] A. Alcorn, Embodied energy and CO_2 coefficients for NZ building materials, Cent. Build. Perform. Res. Vic. Univ. Wellingt. (2001) (Available at), ⟨www.victoria.ac.nz/cbpr/documents/pdfs/eecoefficients⟩.

[51] B. Reddy, K. Jagadish, Embodied energy of common and alternative building materials and technologies, Energy Build. 35 (2003) 129–137, https://doi.org/10.1016/S0378-7788(01)00141-4.

[52] M.E. Boesch, S. Hellweg, Identifying improvement potentials in cement production with life cycle assessment, Environ. Sci. Technol. 44 (2010) 9143–9149, https://doi.org/10.1021/es100771k.

[53] D.L. Kong, J.G. Sanjayan, Effect of elevated temperatures on geopolymer paste, mortar and concrete, Cem. Concr. Res. 40 (2) (2010) 334–339, https://doi.org/10.1016/j.cemconres.2009.10.017.

[54] Office of Energy Efficiency, Energy consumption benchmark guide, Cement Clinker Production, 2001. Available at ⟨https://www.nrcan.gc.ca/sites/www.nrcan.gc.ca/files/oee/pdf/publications/industrial/BenchmCement_e.pdf⟩.

[55] N.P. Rajamane, M.C. Nataraja, N. Lakshmanan, J.K. Dattatreya, D. Sabitha, Sulphuric acid resistant, eco-friendly concrete from geopolymerisation of blast furnace slag, Indian J. Eng. Mater. Sci. 19 (2012) 357–367 (Available at), ⟨http://nopr.niscair.res.in/bitstream/123456789/15164/1/IJEMS%2019%285%29%20357-367.pdf⟩.

[56] A. Adesina, Performance and sustainability overview of sodium carbonate activated slag materials cured at ambient temperature, Res. Environ. Sustain. 3 (2021) 10016, https://doi.org/10.1016/j.resenv.2021.100016.

[57] E. Jamieson, B. McLellan, A. van Riessen, H. Nikraz, Comparison of embodied energies of Ordinary Portland Cement with Bayer-derived geopolymer products, J. Clean. Prod. 99 (2015) 112–118, https://doi.org/10.1016/j.jclepro.2015.03.008.

[58] W. Langer, Sustainability of aggregates in construction, in: J. Khatib (Ed.), Sustainability of Construction Materials, Woodhead Publishing Limited, Cambridge, 2009, pp. 1–30.

[59] K.H. Yang, J.K. Song, K.I. Song, Assessment of CO_2 reduction of alkali-activated concrete, J. Clean. Prod. 39 (2013) 265–272, https://doi.org/10.1016/j.jclepro.2012.08.001.

[60] Australian ANGGA, Natl. Greenh. Gas. Acc. (2013) (Available from), ⟨http://www.climatechange.gov.au/⟩.

[61] M. Fawer, M. Concannon, W. Rieber, Life cycle inventories for the production of sodium silicates, Int. J. Life Cycle Assess. 4 (4) (1999) 207–212, https://doi.org/10.1007/BF02979498.

[62] K.T. Kellenberger, D. Althaus, N. Jungbluth, Life cycle inventories of building products, Final Rep. ecoinvent data v2. 0 No. 7, Dubendorf, CH (2004).

[63] O.M. Althaus, P.A. Althaus, M. Chudacoff, R. Hischier, N. Jungbluth, Life Cycle Inventories of Chemicals, Final Rep. ecoinvent data v2. 0 No. 8., Dübendorf, CH (2007).

[64] R. Zah, R. Hischier, Life cycle inventories of detergents, Final Rep. ecoinvent data v2. 0, No. 12, Dübendorf, CH (2007).

[65] H. Pervez, Y. Ali, A. Petrillo, A quantitative assessment of greenhouse gas (GHG) emissions from conventional and modular construction: a case of a developing country, J. Clean. Prod. 294 (2021), 126210, https://doi.org/10.1016/j.jclepro.2021.126210.

[66] I.Z. Bribian, A.V. Capilla, A.A. Uson, Life cycle assessment of building materials: comparative analysis of the energy and environmental impact and evaluation of the ecoefficiency improvement potential, Build. Environ. 46 (2011) 1133–1140, https://doi.org/10.1016/j.buildenv.2010.12.002.

[67] R. Bajpai, K. Choudhary, A. Srivastava, K.S. Sangwan, M. Singh, Environmental impact assessment of fly ash and silica fume based geopolymer concrete, J. Clean. Prod. 254 (2020), 120147, https://doi.org/10.1016/j.jclepro.2020.120147.

[68] A. Adesina, S. Das, Mechanical performance of engineered cementitious composite incorporating glass as aggregates, J. Clean. Prod. 260 (2020), 121113, https://doi.org/10.1016/j.jclepro.2020.121113.

[69] National Energy Board, Canada's adoption of renewable power sources energy market analysis, 2017, pp. 27. Available at ⟨https://www.cer-rec.gc.ca/en/data-analysis/energy-commodities/electricity/report/2017-canadian-adoption-renewable-power/2017cnddptnrnwblpwr-eng.pdf⟩.

[70] C. Ma, G. Long, Y. Shi, Y. Xie, Preparation of cleaner one-part geopolymer by investigating different types of commercial sodium metasilicate in China, J. Clean. Prod. 201 (2018) 636–647, https://doi.org/10.1016/j.jclepro.2018.08.060.

[71] K.R. O'Brien, J. Menache, L.M. O'Moore, et al., Impact of fly ash content and fly ash transportation distance on embodied greenhouse gas emissions and water consumption in concrete, Int. J. Life Cycle Assess. 14 (7) (2009) 621–629, https://doi.org/10.1007/s11367-009-0105-5.

[72] R. Kumar, Effects of high-volume dolomite sludge on the properties of eco-efficient lightweight concrete: microstructure, statistical modelling, multi-attribute optimization through Derringer's desirability function, and life cycle assessment, J. Clean. Prod. 307 (2021), 127107, https://doi.org/10.1016/j.jclepro.2021.127107.

[73] E.R. Teixeira, R. Mateus, A.F. Camoes, L. Bragança, F.G. Branco, Comparative environmental lifecycle analysis of concretes using biomass and coal fly ashes as a partial cement replacement material, J. Clean. Prod. 112 (2016) 2221–2230, https://doi.org/10.1016/j.jclepro.2015.09.124.

[74] K.K. Patil, C.D. Wolf, S. Chin, J. Ochsendorf, A.E. Hajiah, A. Al-Mumin, O. Büyüköztürk, Impact of Embodied Energy on materials/buildings with partial replacement of ordinary Portland Cement (OPC) by natural Pozzolanic Volcanic Ash, J. Clean. Prod. 177 (2018) 547–554, https://doi.org/10.1016/j.jclepro.2017.12.234.

[75] J. Yu, H.L. Wu, D.K. Mishra, G. Li, C.K.Y. Leung, Compressive strength and environmental impact of sustainable blended with high-dosage Limestone and Calcined Clay (LC2), J. Clean. Prod. 278 (2021), 123616, https://doi.org/10.1016/j.jclepro.2020.123616.

[76] A. Dal Pozzo, L. Carabba, M.C. Bignozzi, A. Tugnoli, Life cycle assessment of a geopolymer mixture for fireproofing applications, Int. J. Life Cycle Assess. 24 (2019) 1743–1757, https://doi.org/10.1007/s11367-019-01603-z.

[77] S.H. Teh, T. Wiedmann, A. Castel, J. de Burgh, Hybrid life cycle assessment of greenhouse gas emissions from cement, concrete and geopolymer concrete in Australia, J. Clean. Prod. 152 (2017) 312–320, https://doi.org/10.1016/j.jclepro.2017.03.122.

[78] Y. Andersson-Skold, S. Thorsson, D. Rayner, F. Lindberg, S. Janhäll, A. Jonsson, M. Granberg, An integrated method for assessing climate-related risks and adaptation alternatives in urban areas, Clim. Risk Manag. 7 (2015) 31–50, https://doi.org/10.1016/j.crm.2015.01.003.

[79] B. Huang, Y. Chen, W. McDowall, S. Turkeli, R. Bleischwitz, Y. Geng, Embodied GHG emissions of building materials in Shanghai, J. Clean. Prod. 210 (2018) 777–785, https://doi.org/10.1016/J.JCLEPRO.2018.11.030.

[80] A. Sagheb, E. Vafaeihosseini, R.P. Kumar, The Role of Building Construction Materials on Global Warming lessons for Architects. National Conference on Recent Trends in Civil Mechanical Engineering, 2011.

[81] K.M. Rahla, R. Mateus, L. Braganca, Comparative sustainability assessment of binary blended concrete using Supplementary Cementitious Materials (SCMs) and Ordinary Portland Cement (OPC), J. Clean. Prod. 220 (2019) 445–459, https://doi.org/10.1016/j.jclepro.2019.02.010.

[82] D.K. Ashish, Concrete made with waste marble powder and supplementary cementitious material for sustainable development, J. Clean. Prod. 211 (2019) 716–729, https://doi.org/10.1016/j.jclepro.2018.11.245.

[83] L. Braganca, R. Mateus, H. Koukkari, Building sustainability assessment, Sustain 2 (7) (2010) 2010–2023, https://doi.org/10.3390/su2072010.

[84] J. Park, J. Yoon, K.H. Kim, Critical review of the material criteria of building sustainability assessment tools, Sustain. (Switz.) 9 (2) (2017), https://doi.org/10.3390/su9020186.

[85] D. Santos, Soda ash, Min. Eng. 58 (2006) 56–57.

[86] K. Shwekat, H.C. Wu, Benefit-cost analysis model of using class F fly ash-based green cement in masonry units, J. Clean. Prod. 98 (2018) 443–451, https://doi.org/10.1016/j.jclepro.2018.06.229.